

Loughborough University
Institutional Repository

*Upper bound on the Andreev
states induced second
harmonic in the Josephson
coupling of
YBa₂Cu₃O_{7-δ}/Nb junctions
from experiment and
numerical simulations*

This item was submitted to Loughborough University's Institutional Repository by the/an author.

Citation: CHESCA, B., SMILDE, H.J.H. and HILGENKAMP, H., 2008. Upper bound on the Andreev states induced second harmonic in the Josephson coupling of YBa₂Cu₃O_{7-δ}/Nb junctions from experiment and numerical simulations. *Physical Review B*, 77 (184510), 6pp.

Metadata Record: <https://dspace.lboro.ac.uk/2134/12891>

Version: Published

Publisher: © American Physical Society

Please cite the published version.

Upper bound on the Andreev states induced second harmonic in the Josephson coupling of $\text{YBa}_2\text{Cu}_3\text{O}_{7-\delta}/\text{Nb}$ junctions from experiment and numerical simulations

B. Chesca,^{1,2,*} H. J. H. Smilde,³ and H. Hilgenkamp³

¹*Department of Physics, Loughborough University, Loughborough LE11 3TU, United Kingdom*

²*Physikalisches Institut-Experimentalphysik II, Universität Tübingen, Auf der Morgenstelle 14, D-72076 Tübingen, Germany*

³*Faculty of Science and Technology and Mesa Institute for Nanotechnology, University of Twente, P.O. Box 217, 7500 AE Enschede, The Netherlands*

(Received 29 January 2008; published 16 May 2008)

Theory predicts that d -wave superconductivity induces a significant second harmonic J_2 in the Josephson current, as a result of zero-energy Andreev states (ZES) formed at the junction interface. Consequently, anomalies such as half-integer Shapiro steps and signatures of period doubling of the dc Josephson current versus magnetic field should be observed. We performed experiments on junctions between untwinned d -wave $\text{YBa}_2\text{Cu}_3\text{O}_{7-\delta}$ and Nb and found no trace of such anomalies although clear evidence of Andreev states formation is provided. These findings do not lead to an observable J_2 . This result combined with extensive numerical simulations put an upper bound on the ZES-induced J_2 of about 0.1% from the first harmonic in the Josephson current for tunneling into the [010] direction and of about 2% for tunneling close to the [110] direction. Our results suggest strong J_2 suppression by diffusive scattering, which is possibly due to nanoscale interface roughness. This is important for proposed (quantum)-electronic device concepts based on the expectation of J_2 .

DOI: [10.1103/PhysRevB.77.184510](https://doi.org/10.1103/PhysRevB.77.184510)

PACS number(s): 74.20.Rp, 74.50.+r, 74.78.Bz

Josephson junctions formed between two superconductors, in which at least one is a d -wave superconductor, are very attractive candidates for the implementation of superconducting qubits in quantum computation¹ or π junctions in Josephson (low-dissipative) digital circuits.² In addition, arrays of such d -wave junctions are of interest as model systems for studying magnetic phenomena—including frustration effects—in Ising antiferromagnets.³ Moreover, d -wave junctions are among the most reliable tools to investigate the unconventional superconducting order parameter in these materials.^{4,5} The physics of d -wave junctions, however, is not fully understood. A key element, namely, the knowledge of the current-phase relation (CPR) of the Josephson current, remains unsettled.⁶ It has been predicted^{7–11} that zero-energy Andreev states (ZES) formed at the d -wave junctions interface are expected to induce a second harmonic Josephson current J_2 in the CPR. For various qubit concepts this J_2 is essential, as a superconducting qubit based on J_2 will have an operating point intrinsically stable and protected against the environmental noise, which will reduce decoherence.¹² Whereas it is now well understood that d wave induces formation of ZES states⁴ and anomalies in the magnetic field dependence of the dc Josephson current,⁵ the existence of J_2 represents an intriguing unconfirmed prediction. In this paper, we address this issue for Josephson junctions made between the d -wave $\text{YBa}_2\text{Cu}_3\text{O}_{7-\delta}$ and Nb. First, we provide evidence for the formation of ZES and the existence of d -wave-induced anomalies in the Josephson current and second, we look for the existence of J_2 . If it exists, this second harmonic component is expected^{7–11} to be highly anisotropic as we change the tunneling orientation in the ab plane reaching its maximum for tunneling close to [110] direction and its minimum for the [100] or [010] directions.

J_2 is expected^{7–11} to produce a deviation from the standard sinusoidal CPR of the Josephson current density J_c ,⁶

$$J_c(\varphi) = J_1 + J_2 = Jc_1 \sin(\varphi) + Jc_2 \sin(2\varphi). \quad (1)$$

Here, φ is the phase difference across the junction. For a purely d -wave order parameter, as we increase θ (the angle in the ab plane between the normal to the junction interface and the [100] crystal axis) starting from 0, J_2 is expected¹⁰ to monotonically increase up to $\theta=45^\circ$ which corresponds to tunneling into the [110] direction. It should then monotonically decrease as we further increase θ from 45° to 90° , corresponding to tunneling into the [010] direction. In particular, for tunneling close to the [110] direction, where J_1 vanishes due to the nodes of the d -wave order parameter, J_2 will dominate the CPR.^{7–11,13–16}

We prepared thin film ramp-edge junctions between 170 nm untwinned $\text{YBa}_2\text{Cu}_3\text{O}_{7-\delta}$ and 150 nm Nb by using a 30 nm Au barrier. The use of untwinned $\text{YBa}_2\text{Cu}_3\text{O}_{7-\delta}$ thin films is especially important because, otherwise, J_2 may be strongly suppressed due to excessive diffusive scattering⁹ at the twin boundaries. Also, J_2 may be averaged out for a badly defined nodal orientation in a twinned film. The junctions are fabricated on the same chip, and the angle θ with the $\text{YBa}_2\text{Cu}_3\text{O}_{7-\delta}$ crystal b axis is varied in units of 5° , so that tunneling can be probed in $360^\circ/5^\circ=72$ different directions in the ab plane (see Fig. 1 of Ref. 17). The growth of untwinned $\text{YBa}_2\text{Cu}_3\text{O}_{7-\delta}$ films,¹⁸ as well as detailed order parameter issues,¹⁷ and ZES-assisted quasiparticle tunneling¹⁹ in these particular junctions are reported elsewhere. All 72 junctions are 4 μm wide.

We first measured the quasiparticle conductance spectra $G(V)$ of all 72 junctions for a wide range of temperatures T (4.2–77 K) and magnetic fields B (0–7 T). A quantitative comparison of some of these measurements with calculations made on the basis of an S_dIS_s tunnel junction model (with the S_s superconductor being Nb and the S_d superconductor being $\text{YBa}_2\text{Cu}_3\text{O}_{7-\delta}$) using quasiclassical techniques was recently

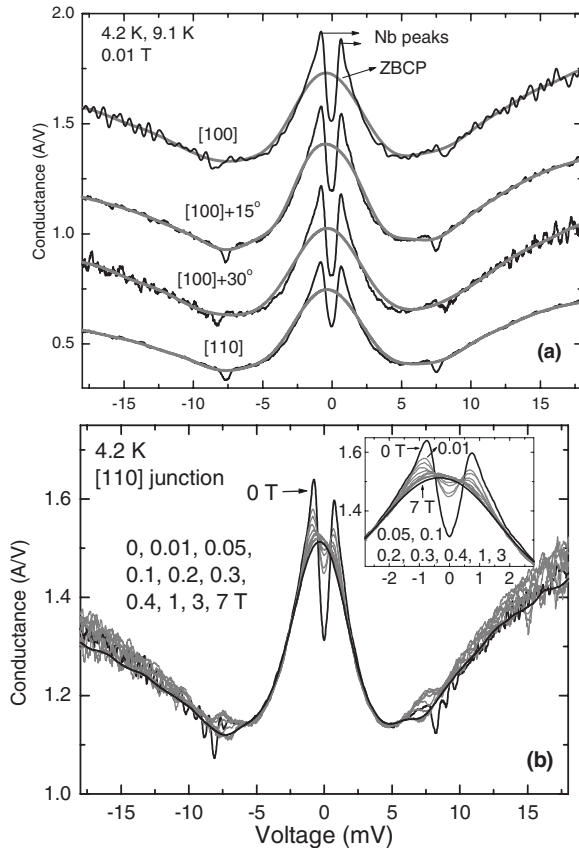


FIG. 1. Representative conductance spectra of (a) four junctions with different tunneling directions at 4.2 K and just below $T_{c,Nb}$, and (b) a [110]-oriented junction for ten different magnetic field values from 0 T (in black) up to 7 T (in black). The inset of (b) shows details of the low voltage spectra.

published.¹⁹ It was found that all observed features are consistent with a convolution of density of states with broadened ZES formed at the $YBa_2Cu_3O_{7-\delta}/Au/Nb$ junction interfaces.¹⁹ Here, we only summarize some of the most important findings from a qualitative point of view. We observed the same qualitative picture independent of the tunneling direction. At 4.2 K and a small B of 0.01 T, which is large enough to completely suppress the dc Josephson current,²⁰ well-defined Nb coherence peaks and a dip at the center of a broadened zero-bias conductance peak (ZBCP) are observed (see Fig. 1). As superconductivity is suppressed in Nb, by increasing T from 4.2 K up to slightly below the critical temperature of Nb ($T_{c,Nb} \approx 9.1$ K) or B from 0.1 T up to slightly below the second critical field of Nb ($B_{c2,Nb} \approx 1.15$ T), the Nb coherence peaks become suppressed and the ZBCP presence gradually manifests. Close to the critical temperature $T_{c,Nb}$ [see Fig. 1(a)] or to 0.4 T [see Fig. 1(b)] no trace is left of the Nb coherence peaks, while the ZBCP is fully developed. That provides clear evidence for the formation of ZES. By increasing T or B even further (from $T_{c,Nb}$ up to 77 K, or B from 0.4 T to $B_{c2,Nb}$ and further to 7 T), however, a significant difference appears between the T and B dependence of $G(V)$. The ZBCP (its amplitude and width) is essentially not affected by an increase in B , while by increasing T , the ZBCP becomes strongly suppressed and wid-

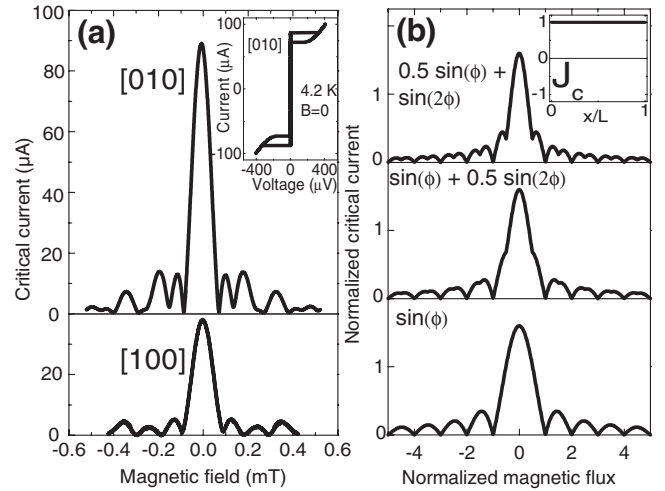


FIG. 2. (a) Measured Josephson current–magnetic field dependences of [010] and [100] junctions. The inset of (a) shows the current–voltage characteristics at $B=0$. (b) Simulation of (a) using three different CPRs; The inset of (b) shows the current density distribution used in the simulations.

ens. In particular, we could not observe any trace of a ZBCP at 77 K. The remarkable insensitivity of $G(V)$ to the tunneling direction strongly suggests the existence of ZES in all tunneling orientations in the ab plane, including the [100] and [010] directions. We believe this is a signature of diffusive reflection or scattering, possibly due to microscopic interface roughness.

To identify J_2 ,^{10,13,15} we first investigate the B dependence of the dc Josephson critical current $I_c(B)$ as a function of the junction orientation [see Figs. 2(a) and 3(a)]. B is applied along the [001] direction. In all cases we should expect a dependence that is close to a Fraunhofer pattern, however, the periodicity of $I_c(B)$ for tunneling close to [110] direction should include signatures of period doubling if J_2 has a significant amplitude. $I_c(B)$ curves were extracted from families of current–voltage characteristics measured for various B values (a typical example is shown in the inset of Fig. 2(a)). The [100] and [010] junctions have an $I_c(B)$ that qualitatively resembles a Fraunhofer pattern [see Fig. 2(a)], suggesting a *homogeneous* distribution of J_c along the junctions. After a quantitative analysis, however, we found that there are small deviations in the measurements from a Fraunhofer pattern which might be associated with a small degree of J_c inhomogeneity. In contrast, for tunneling close to the [110] direction, i.e., [110], $[110^\circ \pm 5^\circ]$ and $[110^\circ \pm 10^\circ]$, $I_c(B)$ strongly deviates from a Fraunhofer pattern [see Fig. 3(a)] and suggests a highly *inhomogeneous* critical current distribution along the junctions. That is due to a junction interface that consists of a multitude of small facets having different sizes and orientations and characterized by alternating signs of the dc Josephson current.²¹ Within this faceted d -wave junction model,^{21,22} one can evaluate various $J_c(x)$ distributions along the junction,¹⁹ as well as various combinations (J_{c1}, J_{c2}) until the simulated $I_c(\Phi/\Phi_0)$ given by

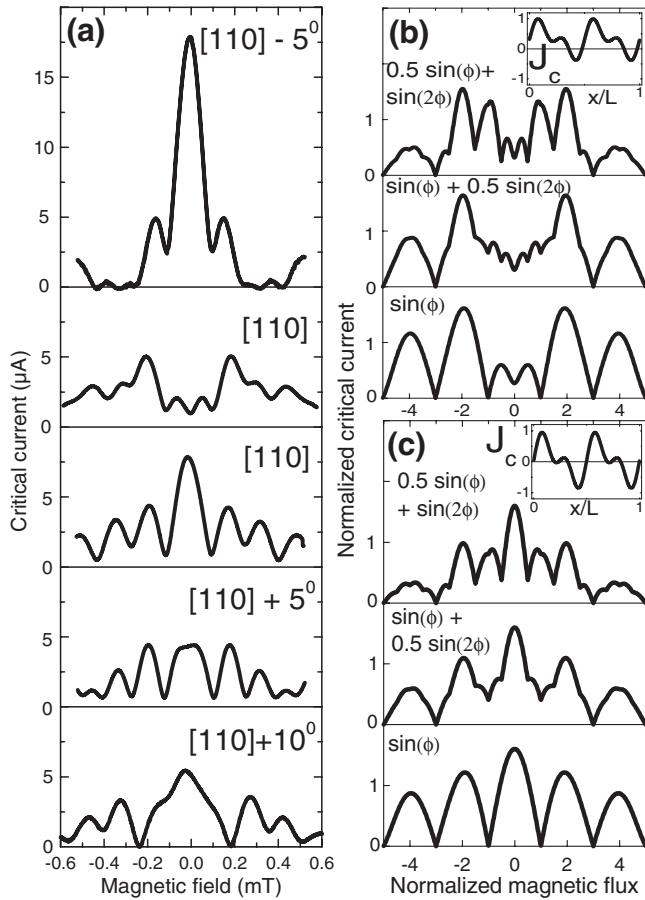


FIG. 3. (a) Measured Josephson current–magnetic field dependences for tunneling close to the [110] direction. (b) Simulation of the second measurement from the top in (a) with three different CPRs; (c) Simulation of the third measurement from the top in (a) using three different CPRs. The insets of (b) and (c) are the current density distributions used in the simulations. The values $\pm 5^\circ$ and $\pm 10^\circ$ are defined with respect to the [110] direction increasing θ from the [010] toward the [100] direction.

$$I_c(\Phi/\Phi_0) = w \max_{\phi_0} \left\{ \int_{-L/2}^{L/2} J_c(x) [J_{c1} \sin(2\pi\Phi/\Phi_0 + \phi_0) + J_{c2} \sin(4\pi\Phi/\Phi_0 + 2\phi_0)] dx \right\} \quad (2)$$

best fits the measured $I_c(B)$. In this, we maximize with respect to the phase ϕ_0 to find $I_c(\Phi/\Phi_0)$. In Eq. (2), w is the junction width, L is the junction length, and Φ/Φ_0 is the normalized magnetic flux applied to the junction with $\Phi = LdB$, where d is the barrier thickness including the London penetration depth in both electrodes. To compare the simulations with the measurements, from the $I_c(B)$ oscillations, we find that one Φ_0 per junction corresponds to approximately 0.1 mT, a value that is independent from the tunneling direction. We cannot simply take the Fourier transform of a measured $I_c(B)$ to find the higher harmonics in the CPR because $J_c(x)$ is not only highly inhomogeneous due to faceting but has a unique and *unknown* pattern for each individual junction. An excellent *quantitative* agreement between the simu-

lated $I_c(\Phi/\Phi_0)$ and the measured $I_c(B)$ can be reached only if rather complicated $J_c(x)$ solutions are being used. Without losing the generality of our conclusions, we found instead that it is preferable to look for a *qualitative* agreement by choosing simpler $J_c(x)$ distributions. To prove the principle of approach, we show simulated $I_c(\Phi/\Phi_0)$ of [010] or [100] junctions [see Fig. 2(b)] and of two [110] junctions [see Figs. 3(b) and 3(c)], whose measured $I_c(B)$'s are presented in Figs. 2(a) and 3(a) [second and third measurements from the top in Fig. 3(a)], respectively. We considered three cases: a purely sinusoidal CPR [$\sin(\phi)$], one dominated by $J_1[\sin(\phi) + 0.5 \sin(2\phi)]$ and one dominated by $J_2[0.5 \sin(\phi) + \sin(2\phi)]$. As far as [100] or [010] junctions are concerned, the best agreement is for a purely sinusoidal CPR with a homogeneous $J_c(x)$ —see Fig. 2(b). Indeed, as soon as J_2 is nonzero, some clear signatures of period doubling (like shoulders or nonzero minima) appear in the simulated $I_c(\Phi/\Phi_0)$ at about $\Phi/\Phi_0 = \pm(2n+1)/2$ (n being an integer). We never observed such features in the measurements. For [110] junctions, by choosing a $J_c(x)$ distribution that changes sign four times (corresponding to four facets per junction), we found that, again, the best qualitative agreement is reached for a purely sinusoidal CPR. By adding a finite J_2 in the simulations, some clear signatures of period doubling appear on the $I_c(\Phi/\Phi_0)$ in the form of additional maxima or singularities in the slope of $I_c(\Phi/\Phi_0)$ (i.e., a shoulder or a kink) as compared to the case of a purely sinusoidal CPR. For instance, if J_2 dominates the CPR, there has to be two additional maxima located in the range $(-\Phi_0, \Phi_0)$ [compare lower plot with upper plot in Figs. 3(b) and 3(c)]. If, on the other hand, J_1 dominates the CPR, two additional maxima [compare lower plot with middle plot in Fig. 3(b)] or two additional kinks or shoulders [compare lower plot with middle plot in Fig. 3(c)] should be observed within the range $(-\Phi_0, \Phi_0)$. For significant values of J_2 (10% or more), similar additional features are visible in the intervals $[-(n+1)\Phi_0, -n\Phi_0]$ and $[n\Phi_0, (n+1)\Phi_0]$ with $n=1, 2, 3$ as well. We have simulated a very large number of different $J_c(x)$ distributions that, to a good degree, are consistent with the $I_c(B)$ measurements of all junctions. We also tried many different (J_1, J_2) combinations and have come to the conclusion that, period-doubling features located at small B fields, if observed experimentally, are unambiguously related to the existence of a significant J_2 . Indeed, if a purely sinusoidal CPR ($J_2=0$) is used to reconstruct the measured $I_c(B)$ then second-harmonic features cannot be reproduced as a result of an accidental interplay between the number of facets, their orientation or size. We have found no trace of such signatures of period doubling for tunneling for any of the junctions measured. Instead, we observed that for tunneling close to the [110] direction [Fig. 3(a)], the total number of maxima or shoulders on the $I_c(B)$ located at low fields within a given interval never exceeds the number obtained for [100] or [010] junctions. In fact, it is usually smaller in high contrast to simulations in Figs. 3(b) and 3(c) that assume a significant J_2 . Therefore, the absence of any signatures of period doubling in the measured $I_c(B)$ strongly indicates that J_2 is negligibly small. To establish an upper limit on J_2 , we first found that in a thermal noise-free environment, such signatures are possible to be resolved in the simulations, even if J_2 is an

infinitesimally small percentage of J_1 . This, however, is not the case in the presence of thermal fluctuations, as thermal noise significantly influences the family of dc current-voltage characteristics measured and, consequently, the $I_c(B)$ measurements. To determine the upper bound on J_2 in the presence of thermal fluctuations, that is the minimum J_2 value needed for J_2 -induced anomalies to be resolved in the $I_c(B)$ measurements, we applied the approach developed in Ref. 23. We found that the upper bound value on J_2 is finite and drastically increases as soon as Josephson coupling energy $J_2\Phi_0$ becomes comparable to $k_B T$ (where k_B is the Boltzmann constant). The calculations show that thermal noise will smear out any J_2 -induced anomalies in the $I_c(B)$ measurements if $J_2\Phi_0/k_B T < 3$. That in turn puts an upper limit on J_2 of about $0.1 \mu\text{A}$ at a measuring temperature of 4.2 K. Since no trace of anomalies has been observed, it means that J_2 should be less than about 0.1% from J_1 for tunneling into the [010] direction and less than about 2% from J_1 for tunneling into a direction close to [110] direction.

A second, independent experiment on J_2 concerns Shapiro steps. It is well known that if the CPR is purely sinusoidal [$Jc_2=0$ in Eq. (1)], microwave (MW) radiation of frequency f will induce Shapiro steps at integer n multiples of the voltage V_0 , satisfying the Josephson voltage-frequency relation $f/V_0=0.486 \text{ GHz}/\mu\text{V}$. If Jc_2 is finite also half-integer Shapiro steps should appear at multiples of $V_0/2$.²⁴ If half-integer Shapiro steps are not observed, then the presence of a significant J_2 in the CPR can be ruled out. We performed a very detailed search in the entire frequency range where integer Shapiro steps could be observed [see also Ref. 25], carefully examining every 10 MHz frequency interval within the 1–20 GHz region. We repeated this approach for all junctions investigated. Typical sets of current-voltage characteristics are shown in Figs. 4(a)–4(c) for three junctions: [100], [110], and [110]– 5° . Well-defined integer Shapiro steps, in accordance with the theoretical expectations, are clearly visible. We detected pronounced integer Shapiro steps up to $n=21$ [as in Fig. 3(a)] or even higher in some cases. We also measured the amplitude of the integer Shapiro steps as a function of the microwave current amplitude. Some typical examples are shown in Figs. 4(d)–4(f) for three junctions: [110], [110]± 5° . We found no trace of half-integer Shapiro steps in any of the junctions, although we paid particular attention to those microwave amplitudes where the integer Shapiro steps or the I_c vanishes and consequently the half-integer Shapiro steps are expected to be most pronounced. In particular, as can be inferred from Figs. 4(d)–4(f), increasing the microwave power first fully suppresses I_c and thereafter, the first integer Shapiro step. However, no signature of the first half-integer Shapiro step is observed. Moreover, the fact that I_c is fully suppressed by microwaves [see Figs. 4(d)–4(f)] is a further confirmation that J_2 is insignificantly small as nonzero minima are expected for I_c in case J_2 has considerable amplitude.²⁴ These observations strongly suggest that J_2 in these junctions is very small. To establish an upper bound on J_2 from these measurements, we applied the approach developed in Ref. 26 for assessing the effect of thermal fluctuations on Shapiro steps and, consequently, for finding the minimum value of J_2 needed for a half-integer Shapiro step to be observed. The upper bound on J_2 found

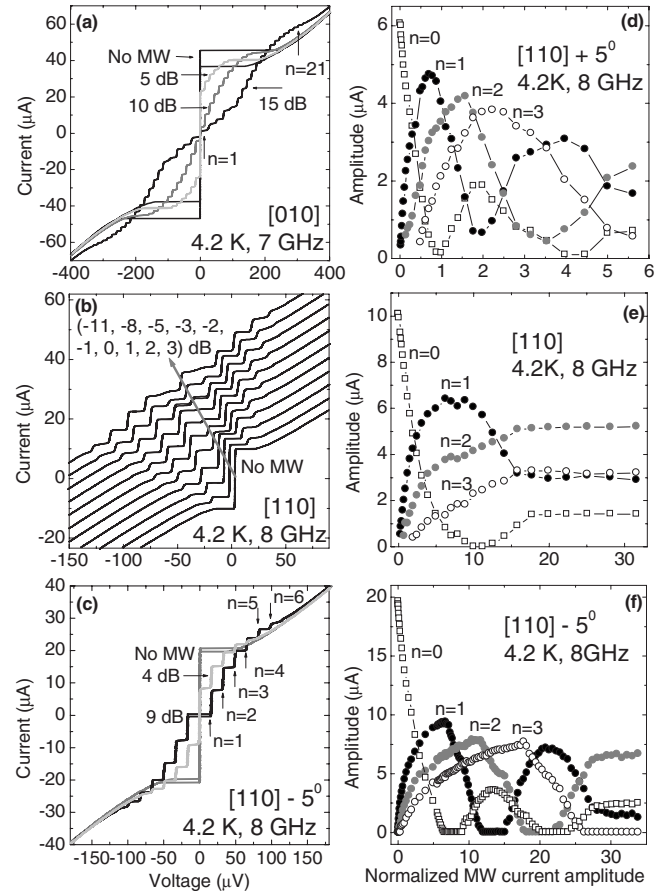


FIG. 4. [(a)–(c)] Integer Shapiro steps (indicated by vertical arrows) at 4.2 K of [010], [110], and [110]– 5° -oriented junctions at different microwave amplitudes. For clarity, the current-voltage characteristics in (b) are shifted in diagonal direction shown by the gray line. [(d)–(f)] Amplitude of the first three integer Shapiro steps and of the critical current versus the normalized microwave-current amplitude for a [110], [110]– 5° , and [110]± 5° junction.

this way was between 0.15% from J_1 (for tunneling into the [010] direction) and 2.5% from J_1 (for tunneling close to the [110] direction). That is slightly higher than the upper bound calculated from $I_c(B)$ measurements. This difference is primarily due to a small I_c suppression observed in the measurements that is caused by an extra source of noise introduced into the system while applying the MW.

As our previous report showed,¹⁹ as far as quasiparticle tunneling is concerned, there is a good quantitative agreement between the measured conductance spectra and calculations made on the basis of an $S_d I S_s$ tunnel junction model using quasiclassical techniques. Looking into the Josephson tunneling, in the frame of a Green's function formalism J_2 is calculated by integrating over all transverse wave vectors,⁹

$$J_2 = \frac{2e}{\pi\hbar} \int_{-\infty}^{\infty} dE f(E) \int_{-\pi/2}^{\pi/2} \frac{d\alpha}{2} \cos \alpha J(\alpha, E), \quad (3)$$

where $J(\alpha, E) = 2\pi |M(\alpha)|^2 E^2 g_{\text{YBCO}}^{\text{eh}}(\alpha, E) g_{\text{Nb}}^{\text{eh}}(\alpha, E) \delta'(E)$, $g_{\text{YBCO, Nb}}^{\text{eh}}(\alpha, E)$ are the pair-correlation functions in the two superconductors, $M(\alpha)$ is the matrix element between Nb

and YBCO, $\delta'(E)$ is the derivative of the Dirac delta function, and α is the angle between a reflected wave and the normal to the junction interface. From Eq. (3), it follows that junction roughness has a dramatic influence on J_2 . For a smooth junction, the tunneling process does not affect the transverse momentum of the quasiparticle and J_2 has to be observed in experiments. We believe our junctions are rough on the scale of a Fermi wavelength. In this case, a quasiparticle in one transverse direction in Nb can get scattered to any transverse direction α in YBCO. This results in an averaging of the pair-correlation functions over different directions α . Since $g_{\text{YBCO,Nb}}^{\text{ch}}(\alpha, E)$ are antisymmetric functions of α ,⁹ this averaging process makes J_2 completely disappear. Our assumption of rough junctions is also consistent with ZES formation in all tunneling orientations in the ab plane including the [100] and [010] directions, in high contrast to the case of smooth junctions.

It has been predicted^{8–11} that J_2 would increase with decreasing temperature and would reach very high values close to 0 K. On the basis of measurements performed in this work, we can only conclude that we did not observe any trace of J_2 at 4.2 K and above, as no data were taken below 4.2 K. It would be of interest to extend such an investigation into the very low temperature range as well.

So far, there have been experimental reports consistent with the presence of a finite second harmonic^{27–29} in various types of twinned $\text{YBa}_2\text{Cu}_3\text{O}_{7-\delta}$ (YBCO) junctions but in none of these cases has the formation of ZES at the junction interface been confirmed. Therefore, its presence cannot be attributed to ZES formation, while there are other alternative mechanisms that may generate it.⁶ Thus, in Refs. 27 and 28, a second harmonic has been observed in structures containing YBCO 45° grain-boundary junctions (GBJs). In Ref. 27, the authors explain its appearance as a result of a very disordered junction interface with many parallel transport channels; some with high-transmissivity and some with low-transmissivity. In a different approach in Ref. 28, the authors

believed the second harmonic in 45° GBJ was due to faceting.²¹ A significant second harmonic is indeed expected³⁰ in a GBJ characterized by an oscillating Josephson critical current density along the junction width, which is the case of 45° GBJ due to a heavily meandering junction interface. Finally, in Ref. 29, the authors concluded on the existence of a second harmonic from the observation of half-integer Shapiro steps in YBCO ramp-edge junctions. It should be pointed out, however, that the observation of half-integer Shapiro steps does *not* necessarily imply that there should be a finite second harmonic in the CPR since there are several other mechanisms that may be responsible for that. Among the most important ones are, a large junction capacitance,³¹ flux trapped in the junctions,³² the synchronized motion of Josephson vortices in long junctions,³³ or the faceting in long grain boundary junctions.³⁰ Additional investigations would be required to rule out all these alternative mechanisms in Ref. 29.

In summary, we provided strong evidence in support of ZES formation in untwinned, d -wave $\text{YBa}_2\text{Cu}_3\text{O}_{7-\delta}/\text{Nb}$ junctions. However, in contrast to the theoretical predictions,^{7,8,10,11,13–16} both $I_c(B)$ and Shapiro step measurements reveal no trace of a ZES-induced Josephson current J_2 . An upper bound has been established for J_2 . We believe that it is scattering due to junction roughness on the scale of a Fermi wavelength that completely suppresses J_2 . Our results therefore suggest that the nature of J_2 in *various* types of d -wave junctions, not only in the ramp-edge junctions investigated here, is more subtle than previously anticipated due to its extreme sensitivity to intrinsic and unavoidable aspects of tunneling phenomena like scattering. Therefore, the observation of a ZES-induced Josephson current may prove to be a very difficult task in experiments. They also suggest that $\text{YBa}_2\text{Cu}_3\text{O}_{7-\delta}/\text{Nb}$ d -wave junctions have a purely sinusoidal CPR, which is essential in taking into consideration their implementation as qubits^{1,12} or π junctions in digital circuits.²

*Corresponding author. b.chesca@lboro.ac.uk

¹L. B. Ioffe, V. Geshkenbein, M. V. Feigel'man, A. L. Fauchère, and G. Blatter, *Nature (London)* **398**, 679 (1999).

²T. Orllepp, Ariando, O. Mielke, C. J. M. Verwijs, K. F. K. Foo, H. Rogalla, F. H. Uhlmann, and H. Hilgenkamp, *Science* **312**, 1495 (2006); E. Terzioglu and M. R. Beasley, *IEEE Trans. Appl. Supercond.* **8**, 48 (1998).

³H. Hilgenkamp, Ariando, H. J. H. Smilde, D. H. A. Blank, G. Rijnders, H. Rogalla, J. R. Kirtley, and C. C. Tsuei, *Nature (London)* **422**, 50 (2003).

⁴C. C. Tsuei and J. R. Kirtley, *Rev. Mod. Phys.* **72**, 969 (2000).

⁵S. Kashiwaya and Y. Tanaka, *Rep. Prog. Phys.* **63**, 1641 (2000).

⁶A. A. Golubov, M. Yu. Kupriyanov, and E. Il'ichev, *Rev. Mod. Phys.* **76**, 411 (2004).

⁷Y. Tanaka and S. Kashiwaya, *Phys. Rev. B* **53**, R11957 (1996).

⁸Y. S. Barash, H. Burkhardt, and D. Rainer, *Phys. Rev. Lett.* **77**, 4070 (1996).

⁹M. P. Samanta and S. Datta, *Phys. Rev. B* **55**, R8689 (1997).

¹⁰Y. Tanaka and S. Kashiwaya, *Phys. Rev. B* **56**, 892 (1997).

¹¹R. A. Riedel and P. F. Bagwell, *Phys. Rev. B* **57**, 6084 (1998).

¹²M. H. S. Amin, A. Y. Smirnov, A. M. Zagorskin, T. Lindstrom, S. A. Charlebois, T. Claeson, and A. Y. Tzalenchuk, *Phys. Rev. B* **71**, 064516 (2005).

¹³Y. Tanaka, *Phys. Rev. Lett.* **72**, 3871 (1994).

¹⁴A. Huck, A. van Otterlo, and M. Sigrist, *Phys. Rev. B* **56**, 14163 (1997).

¹⁵A. Zagorskin, *J. Phys.: Condens. Matter* **9**, L419 (1997).

¹⁶T. Lofwander, V. S. Shumeiko, and G. Wendin, *Phys. Rev. B* **62**, R14653 (2000).

¹⁷H. J. H. Smilde, A. A. Golubov, Ariando, G. Rijnders, J. M. Dekkers, S. Harkema, D. H. A. Blank, H. Rogalla, and H. Hilgenkamp, *Phys. Rev. Lett.* **95**, 257001 (2005).

¹⁸J. M. Dekkers, G. Rijnders, S. Harkema, H. J. H. Smilde, H. Hilgenkamp, H. Rogalla, and D. H. A. Blank, *Appl. Phys. Lett.* **83**, 5199 (2003).

¹⁹B. Chesca, D. Doenitz, T. Dahm, R. P. Huebener, D. Koelle, R.

- Kleiner, Ariando, H. J. H. Smilde, and H. Hilgenkamp, *Phys. Rev. B* **73**, 014529 (2006).
- ²⁰The quasiparticle measurements were taken in an electrically-unshielded environment. The relatively small Josephson current of about $1 \mu\text{A}$ of junction [110] was fully suppressed by the unscreened environmental electronic noise and therefore was not visible in the quasiparticle data even at $B=0$ [see Fig. 1(b)].
- ²¹H. Hilgenkamp, J. Mannhart, and B. Mayer, *Phys. Rev. B* **53**, 14586 (1996).
- ²²R. G. Mints and V. G. Kogan, *Phys. Rev. B* **55**, R8682 (1997).
- ²³B. Chesca, *J. Low Temp. Phys.* **112**, 165 (1998).
- ²⁴L.-E. Hasselberg, M. T. Levinsen, and M. R. Samuelsen, *J. Low Temp. Phys.* **21**, 567 (1975); K. H. Gundlach and J. Kadlec, *Phys. Lett.* **63A**, 149 (1977); R. Kleiner, A. S. Katz, A. G. Sun, R. Summer, D. A. Gajewski, S. H. Han, S. I. Woods, E. Dantsker, B. Chen, K. Char, M. B. Maple, R. C. Dynes, and John Clarke, *Phys. Rev. Lett.* **76**, 2161 (1996).
- ²⁵B. Chesca, H. J. H. Smilde, and H. Hilgenkamp, *J. Phys.: Conf. Ser.* **97**, 012095 (2008).
- ²⁶B. Chesca, *J. Low Temp. Phys.* **116**, 167 (1999).
- ²⁷T. Lindstrom, S. A. Charlebois, A. Y. Tzalenchuk, Z. Ivanov, M. H. S. Amin, and A. M. Zagoskin, *Phys. Rev. Lett.* **90**, 117002 (2003).
- ²⁸E. Il'ichev, V. Zakosarenko, R. P. J. Ijsselsteijn, V. Schultze, H. G. Meyer, H. E. Hoenig, H. Hilgenkamp, and J. Mannhart, *Phys. Rev. Lett.* **81**, 894 (1998); E. Il'ichev, V. Zakosarenko, R. P. J. Ijsselsteijn, H. E. Hoenig, V. Schultze, H. G. Meyer, M. Grajcar, and R. Hlubina, *Phys. Rev. B* **60**, 3096 (1999).
- ²⁹H. Arie, K. Yasuda, H. Kobayashi, I. Iguchi, Y. Tanaka, and S. Kashiwaya, *Phys. Rev. B* **62**, 11864 (2000).
- ³⁰R. G. Mints, *Phys. Rev. B* **57**, R3221 (1998).
- ³¹C. A. Hamilton and E. G. Johnson, Jr., *Phys. Lett.* **41A**, 393 (1972).
- ³²E. A. Early, A. F. Clark, and K. Char, *Appl. Phys. Lett.* **62**, 3357 (1993).
- ³³D. Terpstra, R. P. Ijsselsteijn, and H. Rogalla, *Appl. Phys. Lett.* **66**, 2286 (1995).